UNIVERSITY OF PLYMOUTH

The Plymouth Student Scientist

Volume 14 | Issue 1 Article 17

2021-07-08

A study of the effect of heat treatments on EN9 steel - grain structure and mechanical properties

Euan McCredie
University of Plymouth

Recommended Citation

McCredie, E. (2021) 'A study of the effect of heat treatments on EN9 steel - grain structure and mechanical properties', The Plymouth Student Scientist, 14(1), pp. 310-340.

This Engineering, Computing and Mathematics Article is brought to you for free and open access by the Journals at PEARL. It has been accepted for inclusion in The Plymouth Student Scientist by an authorized editor of PEARL. For more information, please contact openresearch@plymouth.ac.uk.

2021

A study of the effect of heat treatments on EN9 steel - grain structure and mechanical properties

McCredie, Euan

McCredie, E. (2021) 'A study of the effect of heat treatments on EN9 steel - grain structure and mechanical properties', The Plymouth Student Scientist, 14(1), pp. 310-340.
http://hdl.handle.net/10026.1/17330

The Plymouth Student Scientist
University of Plymouth

A study of the effect of heat treatments on EN9 steel - grain structure and mechanical properties

Euan McCredie

Project Advisors:
Dr. A.M. Cree, School of Engineering, Computing and Mathematics, RYB019, Reynolds, Drake Circus, PL4 6DX.

Dr. D. Haspel, School of Engineering, Computing and Mathematics, EMC, Brunel Labs, Drake Circus, PL4 8AA.

Abstract
Medium carbon steel 070M55, also known as EN9 or AISI/SAE 1055, was heat treated with five different heat treatment procedures to promote varying microstructures resulting in enhanced properties of the metal. The aim of this study is to investigate the effect of different heat treatment procedures on a medium carbon steel, regarding the grain microstructure and mechanical properties. Different heat treatment procedures were researched, and five different methods were chosen. The five procedures were normalising, quenching, and tempering at 250°C, 450°C and 650°C. Additionally, all the tempered specimens were quenched before being raised to their designated temperatures. An Instron 5582 was set to record the tensile modulus (E), tensile stress (σ), and tensile strain (ε) every 0.1 seconds, with the crosshead speed set at 5mm/min. Sudden impact energy absorption, or toughness, was tested on an Avery 6703 Charpy impact machine. The Vicker's hardness was tested on a Buehler MicroMet 5104 using a 10N force.

The test measured the hardness every mm, starting at 0.5mm from the centre left of the specimen to centre right. The EBSD specimens were then mounted in a Buehler SimpliMet 2000 hot mould press and polished to 1000 FEPA grit. The Covid-19 pandemic prevented further development on the microscopy; however, the specimens would have been processed as follows: further polishing with diamond solutions would have been completed before Colloidal Silicia was applied and then finished with a Vibromet. The EBSD microscopy would have then been completed using a JEOL 6610 VP-SEM with Aztec analysis software. The microscopy would have been used to measure the grain size and identify the phases and orientation, before relating the mechanical data to the microscopy data. It was found that a higher tempering temperature correlated to a greater ductility and toughness of the medium carbon steel. There was an additional average of 47.1J of energy absorbed between a 250°C temper and a 450°C one, and then again to a 650°C temper. It was also found that heat treating medium carbon steel does not significantly affect the tensile modulus. The Hall-Petch relation applies to EN9 steel which indicates a positive increase of yield stress to the finer the grains. However, this is less evident when relating the grain size to tensile strength.

Keywords: EN9 steel, AISI/SAE 1055, heat treatments, grain structure, microstructures, tempering, tensile strength, grain size.

Introduction

There are many different heat treatment procedures that all alter the grain structure and mechanical properties of steel respective to procedure.
Steel is widely considered to be a “wonder metal”. This is due to the material’s excellent flexibility in metal working and heat treatment, enabling a wide range of variety of mechanical, physical, and chemical properties (Boyer, 1984). Medium carbon steels have 0.30%-0.60% carbon. They have applications where the strength demands cannot be supplied by low carbon steel which has a carbon content of <0.30% (Kalpakjian & Schmid, 2003). These applications include gears and machining parts. The higher the percentage carbon that the steel has the greater the strength, hardness, and wear resistance. However, the brittleness of the metal also increases (Kalpakjian & Schmid, 2003). Brittleness is seen as a limitation as this results in little deformation before failure and very poor impact toughness. Medium carbon steels, which are the focus of this study, contain magnesium, silicon, phosphorus, and sulphur in addition to carbon (Boyer, 1984).

During the heating of a carbon steel past the eutectoid temperature, the grain structure transforms into austenite, which has a face centred cubic crystalline structure (FCC). Once the crystalline structure becomes FCC, space opens for carbonite atoms to dissolve into the lattice. Rapid cooling or quenching is then applied to the metal. This cooling results in the FCC crystalline structure transforming into a BCC structure. However, because the cooling is rapid there is no time for the carbon to diffuse out of the lattice. The result is carbonite atoms trapped in the lattice which reduces the dislocation motion, leading to limited slip of the atoms and so a harder and stronger material is created (Technical-Tidbits, 2010).

The grain structure of a crystal involves the grain size, orientation, boundary conditions and phase of metal. Each of these individual categories of grain structure can affect the hardness, ductility, strength, and all other properties of the metal. Grain size has a massive effect on the mechanical properties of a metal, as the smaller the grains are, the larger the dislocation density. Practical uses of changing the grain structure can be used in industry to alter the properties of a metal so it fits the specification. Before the structural change of the metal was possible it would have had less than ideal properties.

Literature Review

EN9 Steel

Emergency Number 9 (EN9) steel, is being used in this study. The carbon content is 0.50% - 0.60%, which is within the range of medium carbon steels of 0.30% to 0.60% (Kalpakjian & Schmid, 2003). The steel has good weldability and machining abilities, which is used in applications which require high strength metal, such as gears and rail tracks. The steel has alternate specification names of: C55, DIN 1.0535, AISI1055 and SAE1055 (TATA-STEEL, 2015). The chemical composition and mechanical properties are presented below in Table 1.

Table 1: Chemical composition of EN9 steel (www.steelexpress.co.uk, 2020).

Chemical composition							
C	Si	Mn	Ni	Cr	Mo	S	P
%wt							
0.5-0.6	0.05-0.35	0.5-0.8	-	-	-	0.06Max	0.06Max

Residual Stress

Residual stress is defined as a stress that remains in a system free of external forces and temperature gradients. These stresses develop due to plastic deformations during machining, nonuniform cooling and phase transformations which occur when cooling.

Phases of Steel

There are many phases of steel which are homogenous states of matter of steel, depending on the chemical composition (www.imetllc.com, 2020). These phases significanly change the mechanical properties of the metal. Different phases of steel are predicted by heat treating steel by the use of phase diagrams.

Quenching

Quenching is process used for the purpose of increasing a metal's hardness and is accomplished by the rapid cooling of an austenitised metal to transform the austenite to martensite. However, martensite is very brittle with very low toughness, ductility, and high residual stress.

Tempering

Tempering is one of the heat treatment processes used in this study, involving reheating quench hardened steel. In steels the process reheats the metal after hardening to a temperature below the eutectoid point for a predetermined amount of time (Boyer, 1984). The temperature of tempering is usually carried out between 250ºC and 650ºC (Callister & Rethwisch, 2014). The purpose of tempering is to relieve the residual stresses in the metal so that the toughness and ductility increases. Toughness and hardness negatively correlate, as the toughness and ductility improve the hardness lessens. This balance is altered depending on the specification and need for the material's purpose.

After a carbon steel is subjected to quenching there is a phase transformation from austenite to martensite. Martensite is very brittle and has few applications, so tempering is needed to increase the toughness and ductility. Through tempering the martensite, a body centred tetragonal (BCT) microstructure, transforms into tempered martensite, α Ferrite + Fe_3C microstructure. During this transformation, a cementite phase is created with stable ferrite. Cementite is very hard and brittle with 6.70wt % carbon (Callister & Rethwisch, 2014). This change in microstructure significantly alters the properties of the steel because the cementite phase acts as reinforcement for the ferrite matrix along the boundaries. These boundaries then have the effect of distorting dislocations during plastic deformation. The ferrite matrix has very good ductile properties and good toughness, allowing for plastic deformation before failure. Due to these transformations, tempered martensite has improved properties when compared to untampered martensite (Callister & Rethwisch, 2014).

The tempered martensite has a more stable microstructure because residual stresses are relieved through the tempering process (Driscoll, 2014). Roberts, Averbach and Cohen, and Lement, Averbach and Cohen discovered that there are three important structural changes that occur at different temperatures during tempering (Roberts, Averbach, & Cohen, 1953) (Lement, Averbach, & Cohen, 1955). During the first stage, at a temperature range of 100ºC to 200ºC, Carbon atoms diffuse out of the supersaturated matrix to form transition carbides. These carbides are very fine rods which increase the toughness by creating martensitic laths. This transition reduces the hardness due to the carbon which is lost.
During the second stage, at a temperature range of 200ºC to 300ºC decomposition of the retained austenite to ferrite and cementite takes place.
The third and final stage, at a temperature range of 250ºC to eutectoid temperature, involves coarsening of cementite particles, and creates spheroidite with the remaining transition carbides. The martensite also coarsens and begins to transform back into ferrite and cementite, with the crystal structure changing back into the BCC structure, resulting in less dislocations and consequently a drop in hardness.

A phenomenon can occur in tempering where the toughness decreases. This is called tempering embrittlement. This can occur in the temperature range of 400º to 600º and can also be the result of isothermal exposure to this temperature (TWI, 2020). Temper embrittlement only occurs in a select category of steels which have particular chemical impurities. These steels have alloying elements of manganese, nickel, or chromium with at least one or more impurities of antimony, phosphorous, arsenic or tin. This mixture of alloying elements and impurities significantly increases the temperature that the ductile to brittle transition happens.
Tempering embrittlement can be avoided by either selecting steels which do not contain the element compositions that lead to embrittlement or by following the procedure of tempering above 575ºC or below 375ºC (Callister & Rethwisch, 2014).

The Hall-Petch Relation

The Hall-Petch relation is a correlation between the material's strength on the inverse root of grain size (Li & Dunstan, 2019). This relationship says in simple terms, the smaller the grains the greater the strength. The equation for the Hall-Petch relation is as follows:

$$\sigma(d) = \sigma_0 + \frac{k_{HP}}{\sqrt{d}} \qquad (1)$$

Where $\sigma(d)$ is the stress at yield, σ_0 is the is the corresponding stress for large crystals, k_{HP} is a material constant and d is the grain size.
This effect of greater strength due to smaller grain size is due to the smaller grains resulting in a greater dislocation density in the material, so the slip of the planes in the microstructure is reduced. This reduced slip means the material has greater strength.

Electron Backscatter Diffraction (EBSD) Microscopy

The use of EBSD microscopy is used for many practices. EBSD is used in visualisation the microstructure of a material or metal.
EBSD microscopy is a scanning electron microscope where an electron beam interacts with a tilted crystalline sample and diffracted electrons create a pattern on a fluorescent screen (www.ebsd.com, 2020).

Grain size is a commonly measured in EBSD microscopy. The individual grains are identified through critical misorientation angle. Once the grains have been identified, an analysis of the individual grains takes place. Mapping of the individual grains presents an image describing individual grain size (Oxford-Instruments, 2020a).

EBSD microscopy is also used to analyse the grain boundary characterisation of a material. The misorientation of the boundaries between grains is used to identify boundary types. The grain boundary characterisation is important to identify, as the boundaries offer information on disrupting dislocations, initiation of corrosion, precipitation of new phases and creep (Oxford-Instruments, 2020a).
EBSD microscopy also offers insight into the phase distribution and fraction in a material. The phases are distributed on a map, with the measure of the phase fraction as well. This allows insight into the makeup of the material that is being tested and the special distributions of the phases. (Oxford-Instruments, 2020a)

EBSD microscopy also allows us to investigate the orientation of the grains in a material. Orientational data of EBSD microscopy is used to identify if there is any preferred orientation in the material. The data is spatially presented on a Euler map or series of inverse pole figure maps (Oxford-Instruments, 2020a). The colour of the grains represents the orientational data.

Aim

The research aim is to examine the effect of heat treatments on medium carbon steel, analysing the grain structure and mechanical properties to discover why and how different treatments result in different properties.

Objectives

To achieve the aim the following objectives were set:

1. Sets of Tensile, Charpy impact and EBSD specimens will be heat treated by one of five heat treatment procedures:
    - Normalising
    - Quenching
    - Quenching then tempering at 250°C
    - Quenching then tempering at 450°C
    - Quenching then tempering at 650°C

2. To extract mechanical data from all specimen sets through tensile, Charpy impact and Vicker's hardness tests.
3. To explore the microstructure where information will be extracted from all specimen sets through EBSD microscopy.
4. To establish correlations between the mechanical and microscopy data, supported by relevant explanations for such correlations.

Methodology

Specimen manufacturing

The steel being researched is medium carbon steel 070M55, also known as EN9 or AISI/SAE 1055. The metal was bought in a cold rolled state from Steel Express Ltd with total dimensions of 76.2 × 6.35 × 1500 (in mm). Test specimens were then designed using Solidworks CAD (Computer aided design). Due to Steel Express Ltd only being able to provide the steel with a thickness of 6.35mm and a limited supply of test material being available, not all specimens were able to be designed to the correct standard dimensions.

The Specimens were manufactured into shape using a Flow Mach 2 waterjet. This cuts the specimens from the steel using water pressurised at 60,000 lb/in^2 (PSI). This method of specimen manufacturing is very quick and easy but has a limitation of poor tolerance of about 1mm. This quick specimen manufacturing method was decided to be the optimum choice, even due to the poor tolerance, because a large total number of 75 specimens was required.
All the specimens were cut in the same direction in which the metal had been rolled. This ensured that there were no mechanical properties altered during testing by the orientation of the source steel.

The Charpy impact test specimens would have been designed in accordance with ISO 148-1 (2016), but the University of Plymouth does not have access to this standard. However, through technician experience and information from Callister's book on Material Science and Engineering (Callister & Rethwisch, 2014), the size of Charpy impact test specimens are 10mm × 10mm × 100mm, with a 45 degree V notch in the centre of the specimen, 2mm deep. This standard size cannot be achieved due to the thickness of the source material, so a pseudo specimen was designed.

This pseudo specimen was 10mm × 6.35mm × 100mm with the standard V notch design. The V notch after manufacturing was not ideal. Due to the poor tolerances of the waterjet the notch was more of a C shape. However, the notch still provided a weakness point for the impact test.The impact specimen's part drawing is presented in Appendix 1 and the practical specimen is presented below.

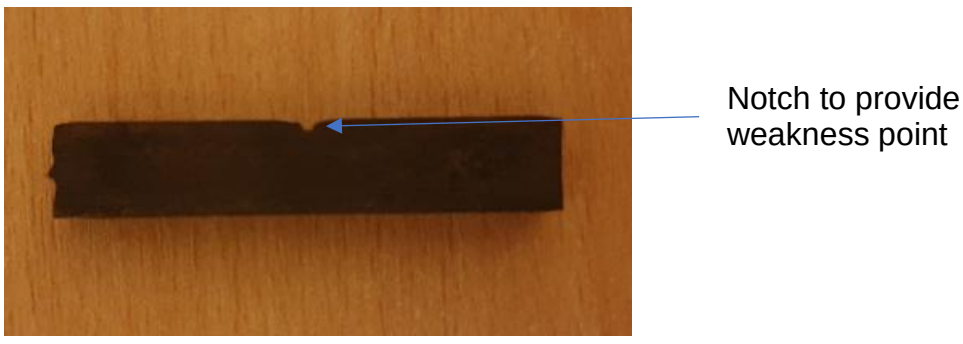

Figure 1: Charpy impact test specimen after manufacturing.

Much like the Charpy impact test specimen, the standard for tensile test specimens and test procedure, ASTM E8/E8M (2016), is also unavailable. However, ASTM E8/E8M – 16A has online access. So, the tensile test specimens were designed to

the metal sub-size dimensions (ASTM-International, 2016). The sub-size specimen dimensions were chosen to ensure enough specimens could be manufactured. The tensile specimen's part drawing is presented in Appendix 2 and the practical specimen is presented below.

Figure 2: Tensile test specimen after manufacturing.

The Vicker's hardness test specimens were designed so that they would be able to be inspected under the EBSD microscope and then be subjected to hardness testing. So, this means that the specimens had to be small enough to fit in the microscope, but still be able to be subjected to hardness tests to present reliable readings. The Vicker's hardness test specimen's part drawing is presented in Appendix 3.

EBSD Microscopy Specimen Preparation

For EBSD microscopy the specimens must be prepared perfectly because diffracted electrons can escape within a few tens of nanometres of the material surface. So, if the surface is slightly deformed, contaminated, or oxidised the EBSD pattern will be suppressed. (ebsd.com, 2020a).

The specimens which have been manufactured as stated in 11.1 must be mounted so they can be polished and examined without becoming dirty through direct human contact. As steel is being used hot mounting, which can reach temperatures of 180°C and denature heat sensitive materials, can be used. Hot mounting is preferred over cold mounting in this study as the quality of hardness of the mound is superior to cold mounting (ebsd.com, 2020b). This is essential as the specimens will have hardness tests conducted while in the mount. Cold mounting which uses materials like epoxy would dampen some of the force and produce unreliable results.

The specimens were then inserted into a Buehler SimpliMet 2000 hot mould press with the mould material, which was a conductive bakelite called KonductoMet. The specimens then need to be ground and polished as the cut surfaces were very rough and suppressed. The Buehler EcoMet 250 is used with Buehler silicon carbide (SiC) papers to achieve this. Starting with a low grit paper to grind, the grit papers used were as follows, 180, 240, 320, 400, 600, 800 and 1000 FEPA with water used as the lubricant. Each succeeding grinding operation grit used no more than a two grit sizes lower, as each step removes material from the previous (www.buehler.co.uk, 2020). Below is the EBSD specimen which has been mounted and polished up to 1000 grit FEPA.

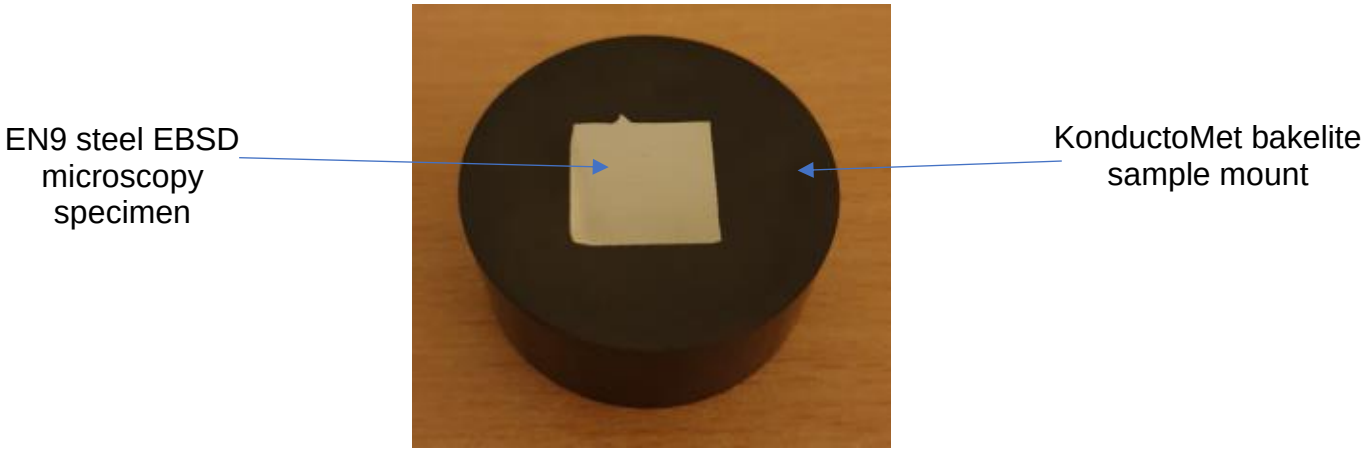

Figure 3: EBSD specimen after mounting and polishing to 1000 grit FEPA.

From this point forward, the description is of what EBSD specimen preparation was planned. Because of the Covid-19 situation all laboratory work was stopped on the 17th March 2020 and no further experimentation could be performed.
The specimens would have been polished with a nylon disc and a 6µm then 3µm Buehler diamond solution to achieve an even greater polish.
Colloidal Silicia would have been applied to the specimens. This is chemo-mechanical polish which combines mechanical polishing with etching, ideal for EBSD specimens as you achieve a damage free surface with little effort (ebsd.com, 2020c).
The specimens would then have been finished with the Vibromet. This uses horizonal vibrations at 7200 cycles per minute which produces less deformation, flatter surfaces and reduced edge rounding, creating a stress free, mirror like surface ready for EBSD microscopy (ebsd.com, 2020c).

Heat Treatment
The procedure for all heat treatments began by separating the specimens into the heat treatment groups. Each group was austenitised, a group at a time, at 830ºC (Boyer, 1984). The specimens had a soak time of 30 minutes. This austenitising time considers the one-hour soak time per inch but adds extra time to ensure full austenitisation. The furnace used to elevate the steel to austenitising temperatures is a Carbolite furnace. During the heating process it was observed to fluctuate in temperature by ± 1°C.

- The normalized group were removed from the furnace after the austenitizing process and left to air cool to room temperature.
- The quenched specimens were removed from the furnace at austenitizing temperature and then quenched in ambient temperature fresh water. During quenching the specimens were moved in a figure of eight pattern, to ensure uniform quenching by avoiding air pockets around the specimens due to water evaporation.
- For the tempering treatments, the specimens were removed from the furnace and quenched, following the quenching procedure laid out. The specimens were then placed back into the furnace at either 250ºC, 450ºC or 650ºC depending on the group. The specimens were left in the furnace at their

constant temperatures for one hour to temper, after this hour they were removed and allowed to air cool to ambient temperature.
- The heat treating was conducted with ambient conditions of 7.5°C and 1005mb.

Mechanical Testing

Charpy Impact Testing

From the five heat treatment groups there were five Charpy impact test specimens requiring testing, resulting in 25 tensile tests to be completed.
Access to the British standard for Charpy pendulum impact test method, ISO 148 – 1:2016, was not available. This resulted in the following test procedure being conducted.
The Chary impact test was conducted on an Avery 6703. The machine collects data by the hammer being raised and locked in place, this position has a potential energy of 300J. From this position the hammer strikes the specimen at 5m/s. Once the hammer has passed through the specimen an arrow points to the new potential energy. The difference between the potential energies is the energy absorbed by the specimen on impact.
This method can be argued to be poor as the test machine does not account for the energies lost as it transfers from the start to stop position, for example, air friction on the hammer.
Impact testing was conducted with ambient conditions of 6.5°C and 1015mb.

Tensile Testing

From the five heat treatment groups there are five tensile specimens requiring testing, resulting in 25 tensile tests to be completed.
Access to the British standard for tensile testing method at room temperature, ISO 6892 – 1:2019, was not available. This resulted in the following test procedure being conducted. The tensile test was conducted on an Instron 5582. The Instron was set to record the Tensile modulus, Tensile stress, and Tensile strain every 0.1 seconds, with the crosshead speed set at 5mm/min. However, the first tensile test was operating at a cross head speed of 2mm/min, this was then increased to 5mm/min due to time constraints. Rectangular clips for an extensometer were used on specimens of size 6mm to 9mm. The extensometer measured the extension then calculated the strain up to 0.002 for every specimen group, apart from the quench group where it was reduced to 0.0015.
Tensile testing was conducted with ambient conditions of 6.5°C and 1015mb.

Vicker's Hardness Testing

One specimen from each of the five heat treatment groups was required to be tested. 15 hardness tests were conducted on each specimen, resulting in a total of 75 hardness tests being performed.
Access to the British standard for Vicker's hardness test method, ISO 6507 – 1:2018, was not available. This resulted in the following test procedure being conducted.
The hardness test was conducted on a Buehler MicroMet 5104 using a 10N force. The hardness value was measured every mm, starting at 0.5mm from the centre left of the specimen to centre right. The Vicker's hardness test specimens were planned to have EBSD microscopy completed on them before hand, but due to the Covid-19 situation this could not happen. As a result, the hardness test specimens were polished up to the 1000 grit stage, then the hardness tests began on them.

Tensile testing was conducted with ambient conditions of 9°C and 1025mb.

EBSD Microscopy

As previously stated, the microscopy could not be completed due to the Covid-19 pandemic halting all research. If this situation had not occurred the methodology for the EBSD microscopy would have been as follows.

The EBSD microscopy would have been completed on a JEOL 6610 VP-SEM (Scanning electron microscope), using Aztec analysis software.

The standard procedure of ASTM E2627 – 13 (2019), Standard Practice for Determining Average Grain Size Using EBSD in Fully Recrystallized Polycrystalline Materials, would have been followed for the microscopy to calculate the average grain size. The microscopy would have also been used to identify the phases and orientation of each specimen. The specimens would be mounted on a pre-tilted holder at 70° and lowered to a working distance of 14mm. An electron beam potential of 15kV and 10nA would have been set and the EBSD camera inserted. The chamber camera and Aztec would have been turned on. The phase parameter would have been added for acquisition. The phases would begin with iron BCC then Iron FCC. The image would then be scanned, and the pattern optimised. A static background would then be setup by drawing an appropriately sized box on the Aztec software. Acquisition parameters would be set, the dwell time would start at 1ms and the mode would be set. The beam would be turned on to check the pattern quality. The solver would then be optimised so that the phases were being sufficiently detected and identified. Then the map data would be acquired which could then be exported. The data then would need to be cleaned, and finally analysed.

Results

Charpy Impact Energy Absorption

Figure 4 shows the energy absorbed for each specimen. The graph presents an error bar for each piece of data, calculated from the standard deviation. Raw data is presented in Appendix 4.

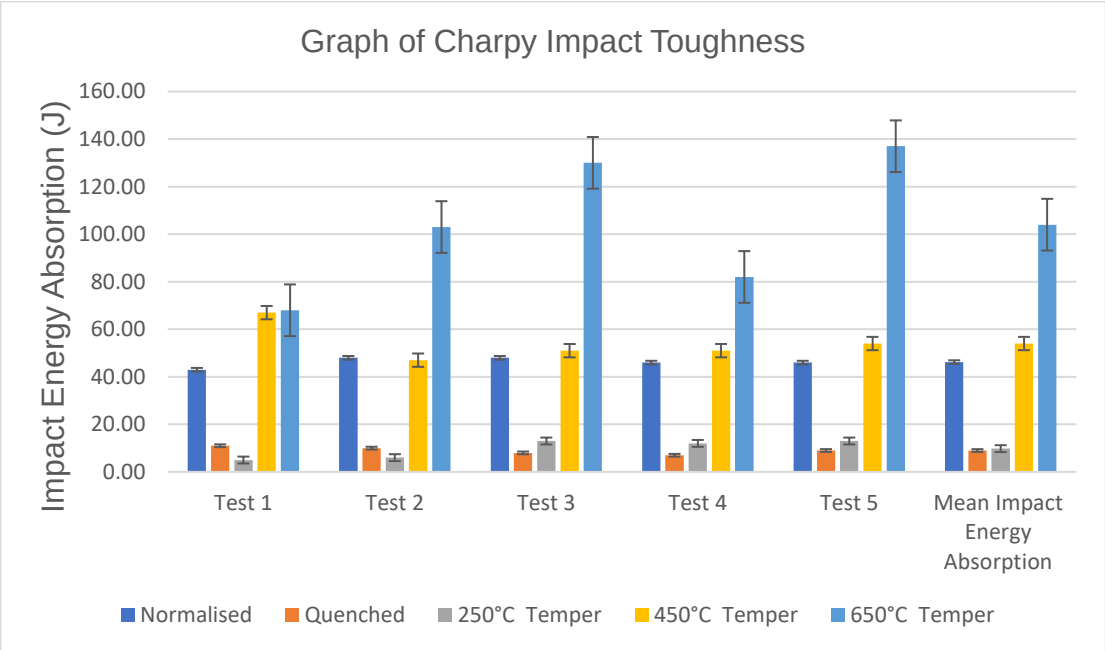

Figure 4: Results of energy absorption from impact testing.

Tensile Modulus

Figure 5 shows the Tensile Modulus of each specimen. The graph presents an error bar for each piece of data, calculated from the standard deviation. Raw data is presented in Appendix 5.

The tests which resulted in a N/A was due to the strain not being recorded as the extensometer slipped on the iron oxide on the specimens.

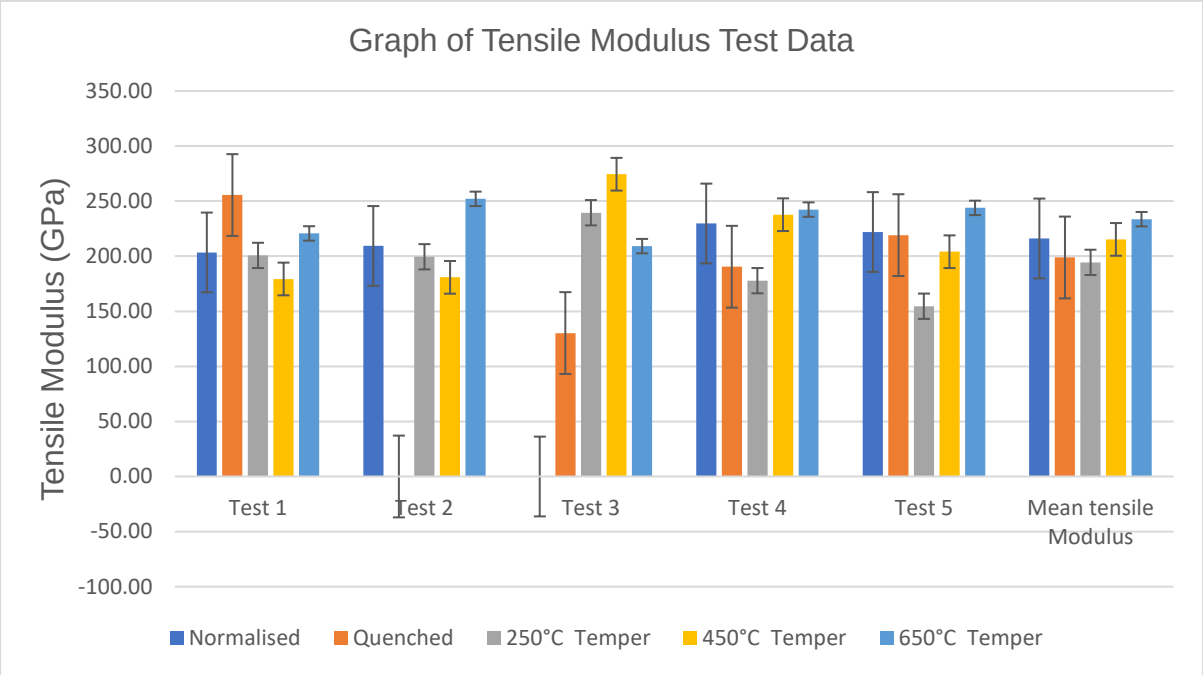

Figure 5: Results of the tensile modulus testing from tensile testing.

Tensile Strength

Figure 6 shows the Tensile strength of each specimen. The graph presents an error bar for each piece of data, calculated from the standard deviation. Raw data is presented in Appendix 6.

The test which resulted in a N/A was due to the Jaws holding the specimen cracking during the test.

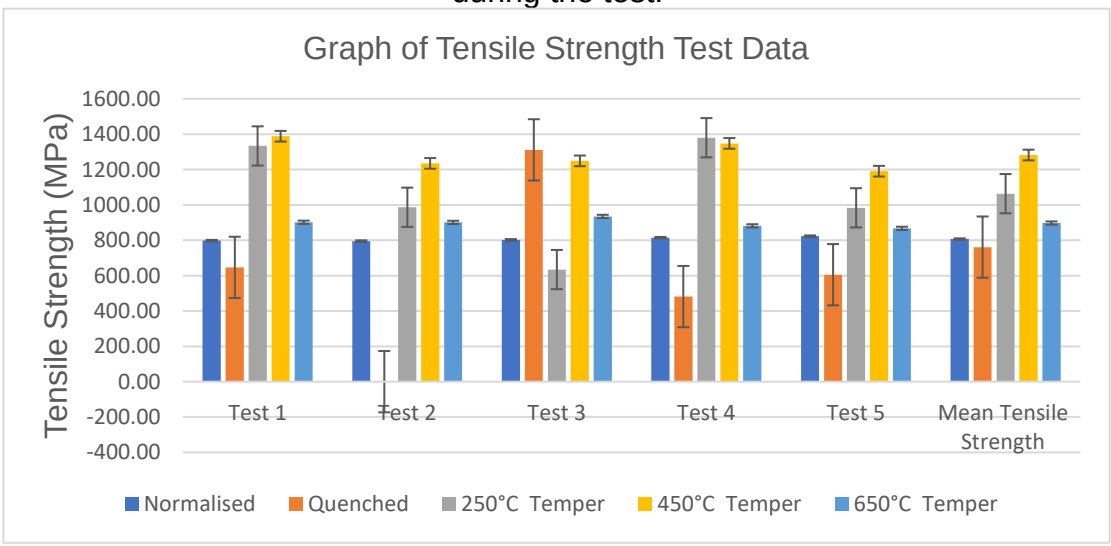

Figure 6: Results of the ultimate tensile strength from tensile testing.

Yield Strength

Figure 7 shows the yield strength of each specimen. The graph presents an error bar for each piece of data, calculated from the standard deviation. Raw data is presented in Appendix 7.
The yield strength was measured by the 0.2% offset method.

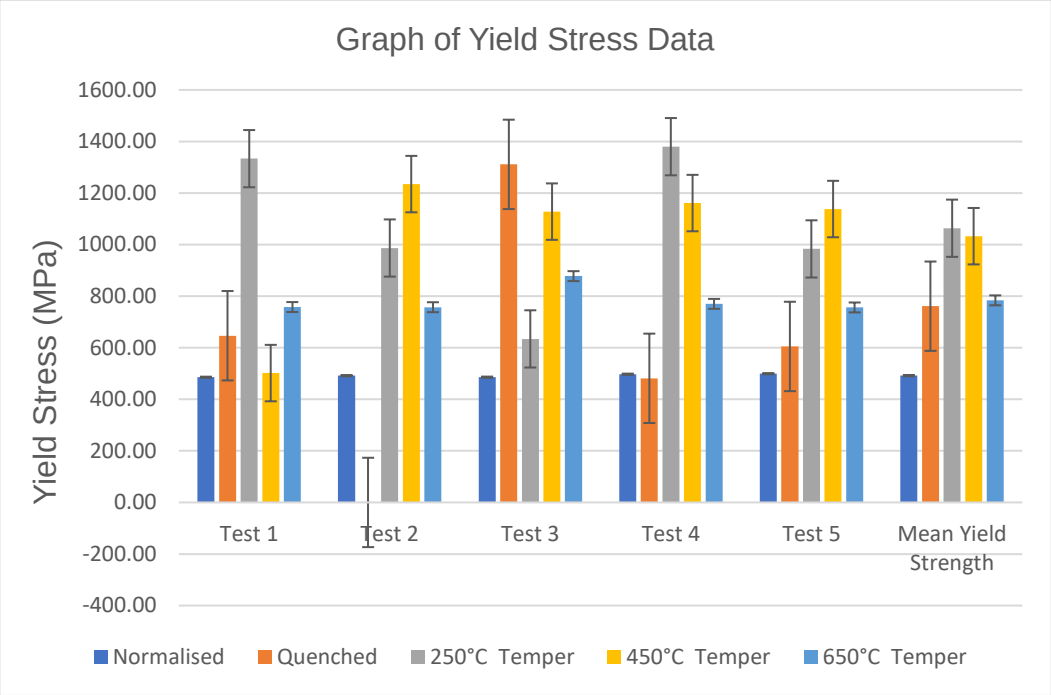

Figure 7: Results of the yield strength from tensile testing.

Vicker's Hardness Values

Figure 8 shows the hardness value of each specimen. The graph presents an error bar for each piece of data, calculated from the standard deviation. Raw data is presented in Appendix 8.
The test which resulted in a N/A was due to the test being conducted on an imperfection on the specimen, which would result in significantly incorrect data.

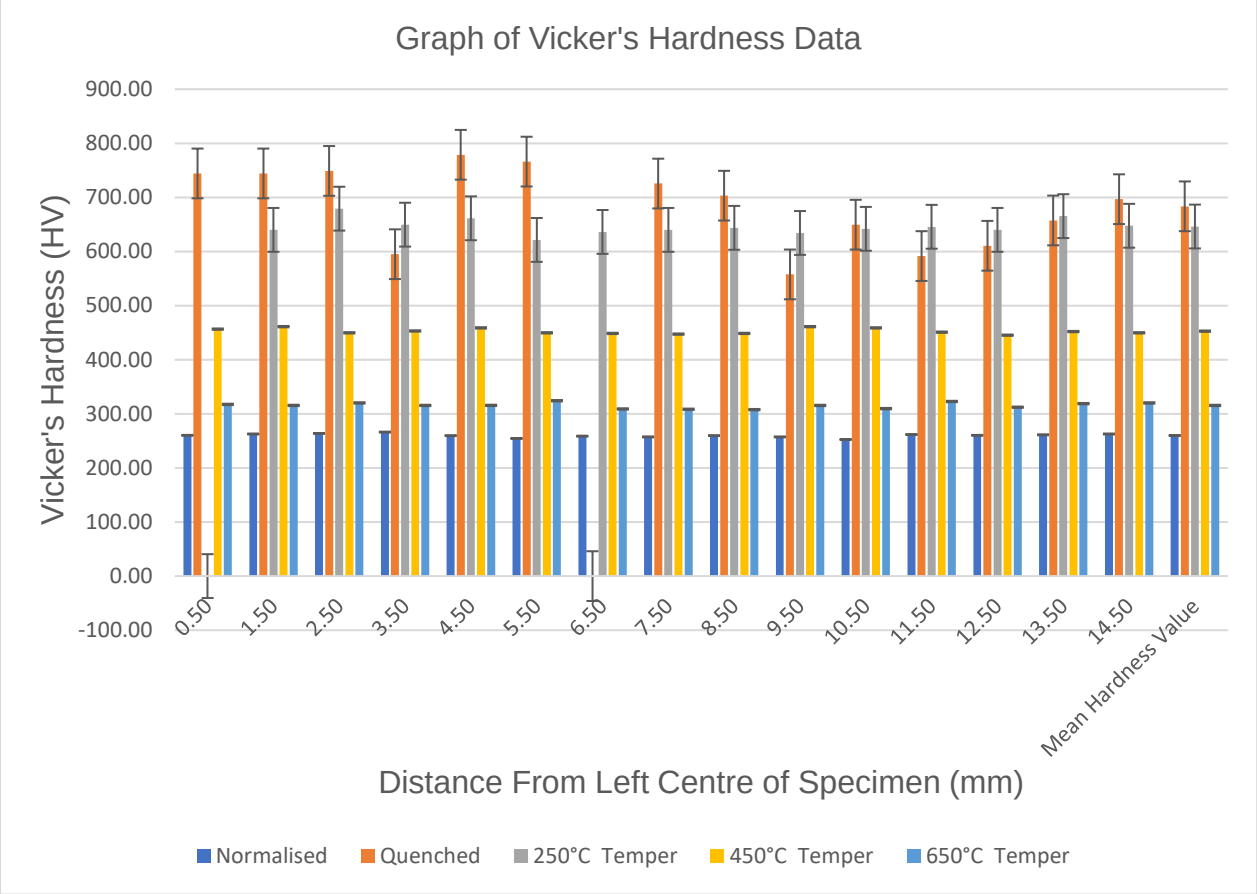

Figure 8: Results of hardness value, from Vicker's hardness testing.

Discussion

Variation of Results

Variation in the results of the data can be due to several reasons, such as underlying and future assumptions and systematic, human, and random errors. These variations can occur at any stage of the study, including manufacturing or preparation, the experimentation methodology or the processing of data and generation of results.
Table 2 shows the possible causes of variation in experimental processes.

Table 2: Possible causes of variation in experimental processes

Procedure	Possible Cause of Variation
Source Metal Assumptions	• The source material was obtained on two separate dates from the same supplier, 24/10/2014 and 07/01/2020. So, an assumption is made that the metal is the same regarding composition, initial grain structure and initial properties. • All the steel is also assumed to have the same composition, grain structure and properties throughout.
Specimen Preparation	• The specimens were assumed to be manufactured ensuring that each specimen had the same dimensions. • The specimens were assumed to have had properties which were affected by during manufacturing, Waterjets can create a lot of friction and heat which could affect the specimens. • The polishing is also assumed to be constant on all specimens, ensuring the surface which Vicker's hardness tests are conducted on are the same.
Heat Treatment	• The specimens were assumed to be in the furnace at constant heat for the same length of time. • The specimens were also assumed to have lost no heat while being transported from furnace to quench bucket. • The quenching is also assumed to be constant every time.
Experimental Procedure	• All the testing equipment is assumed to perform the same for every test. • The equipment is also assumed to be correctly calibrated.
Data Processing	• The raw data is simplified to four decimal points. • The data is simplified and rounded to a maximum of four decimal points.

Coefficient of Variation

The coefficients of variations of each group from each experiment was processed to produce an average coefficient of variation for each heat treatment group. The highest variation was in the quenched group with an average value of 22.88%. This was followed, in decreasing order, by 250°C temper, 650°C temper, 450°C temper then normalised, with respective values of 19.59%, 9.15%, 9.12% and 1.31%.
The significant increase of percentage variation in the quenched and 250°C temper groups is likely due to the quenching process being extremely non-uniform. This quenching process has the potential to evaporate water around the specimen which prevents constant uniform cooling of the metal. This results in different cooling times, which results in some locations creating martensite from the quick cooling, and some location producing Bainite because there is a lengthened cooling. The lengthened cooling allows for carbon to diffuse out of the FCC crystal structure resulting in a different phase of metal and mechanical properties.
To try and reduce this effect and increase the coefficient of variation, a quenching oil should be used. The oil does not evaporate when in contact with a hot specimen, which ensures uniform cooling.

The 450°C temper, 650°C temper and normalised groups had much more accurate coefficients of variation. For the two tempering groups the medium and hot tempering processes likely allowed the microstructure to diffuse some carbon out of the high concentration point of the steel to the less, which created a steel which was more uniform in structure and mechanical properties. The 250°C temper would have a tempering temperature which was too low to allow this to happen in the one hour time frame.
It would be sensible to believe that a longer heat treatment process, would produce a lower the coefficient of variation, although more research would have to be completed to confirm this.

Charpy Impact Test

From the Charpy impact test data it can be observed that the average quenched specimen has the lowest energy absorption of all the groups, 9J of energy being absorbed. The reason for this is the same as to why the quenched specimens have such a high hardness. The martensite is so hard and brittle that the metal can only plasticly deform a tiny amount before failure.
The tempered specimens have higher energy absorption than the quenched specimens, because after the tempering process the microstructure consists of small and evenly dispersed cementite particles in a ferrite matrix (Callister & Rethwisch, 2014). The ferrite phase is very ductile, so the greater the ferrite-cementite phase the softer and tougher the material is.

The highest energy absorption is from the 650°C tempered specimen, with an average of 104J being absorbed. This is the highest because as the tempering temperature increases the cementite particles coalesce and grow which results in increased ferrite and so increased toughness (Kalpakjian & Schmid, 2003).
The slow cooling of normalisation creates pearlite which is a grain structure which consists of small round grains of ferrite and cementite (www.twi-global.com, 2020). The large amount of ferrite explains the average energy absorption is 46.2J. This could be lower than that of the 650°C temper specimens because the pearlite has

finer grain boundaries compared to the tempered steel resulting in a lower concentration of ferrite and so less tough and ductile properties.
The 250°C specimens have energy absorption only 0.8J greater than the quenched specimens. This is due to there being such a small diffusivity coefficient, because the temperature is too low. This is shown by a form of Arrhenius equation presented below:

$$D = D_0 \times exp\left(-\frac{Q}{RT}\right) \qquad (2)$$

Where D is the carbon diffusivity, D_0 is the diffusivity coefficient, Q is the activation energy, R is the gas constant, and T is absolute temperature (Lee, Matlock, & Van Tyne, 2011). For the energy absorption of the 250°C specimen to increase at that temperature, the specimens will have to be tempered much longer than one hour.
Figure 9 presents the relationship between hardness and toughness of the experimental data.
Finally, due to there being a positive correlation between tempering temperature and toughness, there is no evidence to support tempering embrittlement.

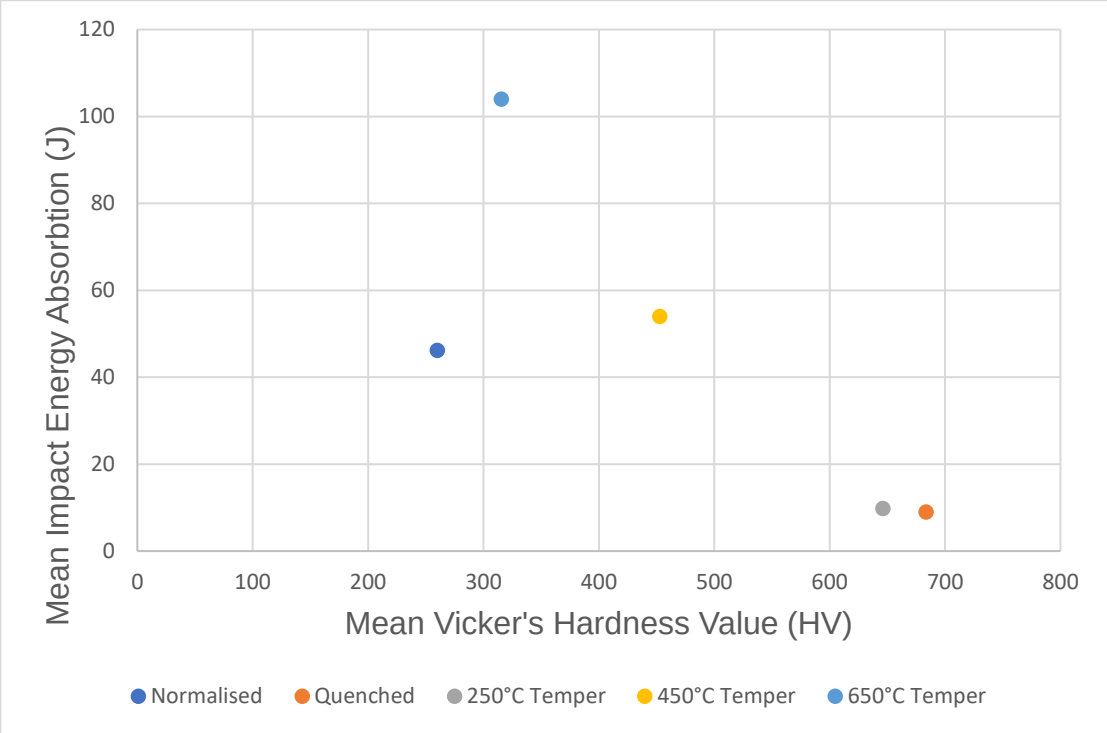

Figure 9: Graph to show the correlation between mean impact energy absorption and hardness value.

Tensile Test

Tensile Modulus

The tensile modulus data from the experiments conducted show that there is no significant effect from heat treatments and hardness on the elastic modulus, as shown in Fig, 15. The blue line represents the trendline.
The modulus does not change significantly. When the yield stress of a specimen increases due to a heat treatment, the strain also increases proportionally so that the

modulus remains constant. This is supported by the elasticity of steel and other metals being dependant on the short range interatomic forces (www.britannica.com, 2020).

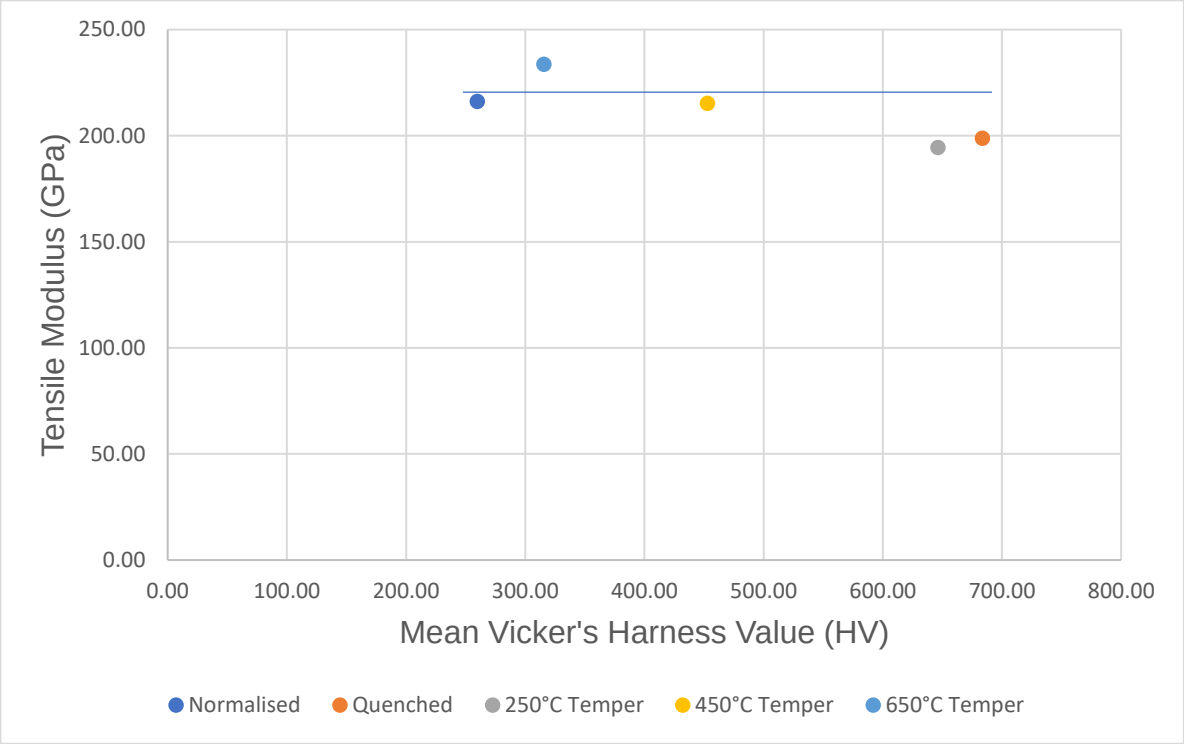

Figure 10: Graph to show the correlation between tensile modulus and hardness value.

Tensile Strength

The tensile strength of a material is assumed to be roughly proportional to the hardness, as shown in Hashemi's paper on the Strength–hardness statistical correlation in API X65 steel (Hashemi, 2010). This relationship is also supported by the ASTM A370 (2019) Standard Test Methods and Definitions for Mechanical Testing of Steel Products (www.metalspiping.com, 2016). The standard is presented in a table. The table presents approximate hardness conversion numbers for non-austenitic steels, where the hardness can be matched to the appropriate and approximate tensile strength. However, the table does not present the tensile strength of steels with hardness greater than 674HV on the Vicker's hardness scale.

The tensile strength of the steel which was tested in this study shows that the tensile strength increases with the hardness, as predicted by Hashemi and the ASTM A370 standard. Although, this relationship is only applicable up to the 250°C temper specimens where the tensile strength begins to decline with hardness. It then declines even further with hardness for the quenched specimen, as shown in Fig. 11. The blue line represents the trendline.

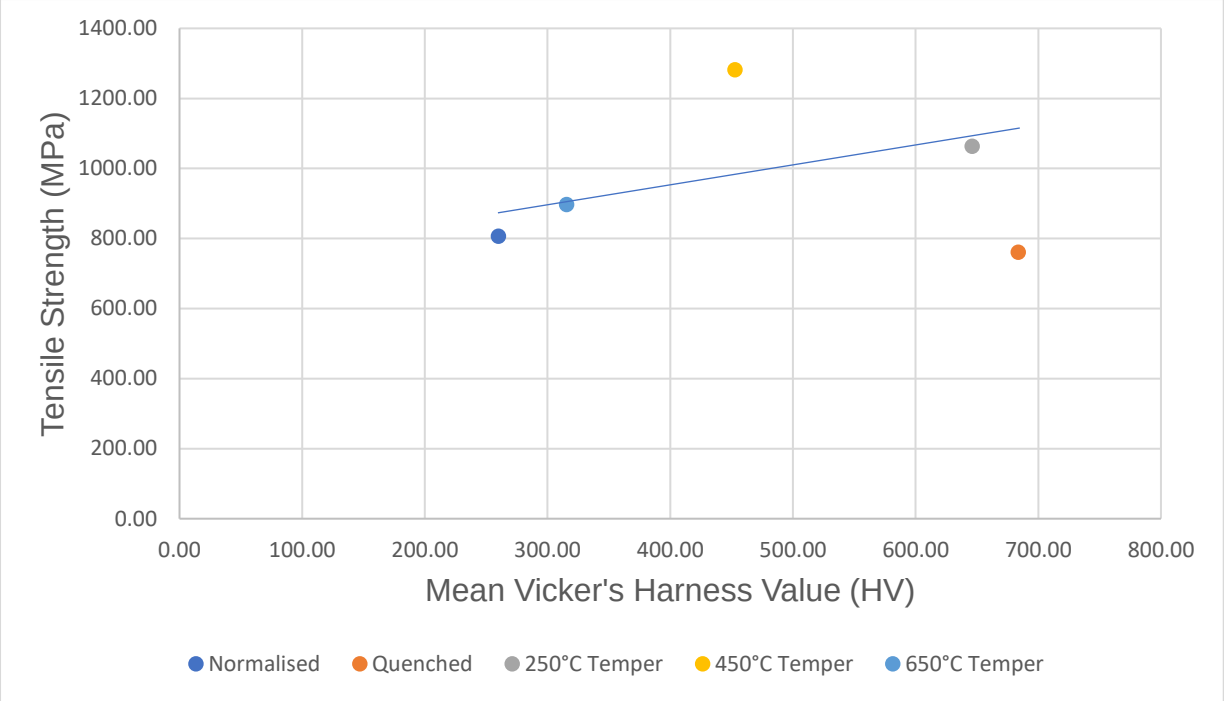

Figure 11: Graph to show the correlation between tensile strength and hardness value.

This does not match the relationship in the other sources, as the tensile strength begins to decline with hardness. The standard approximate hardness to strength data from ASTM A370 does not show the strength for steels with the same hardness as the quenched specimen, so it could be assumed that the strength begins to decline when the steel becomes so brittle that it fails with minimal stress and deformation. It could also be argued that the experimental data could be incorrect, both the 250°C temper and quenched specimens had the largest coefficient of variations with 19.5861% and 22.8844% respectively.
A repeat of the study with a greater number of test specimens would bring greater clarity to the data.

Yield Strength
From the experimental test data, the correlation between hardness and yield strength is much greater than that to tensile strength, as shown on Fig. 12. The blue line represents the trendline.

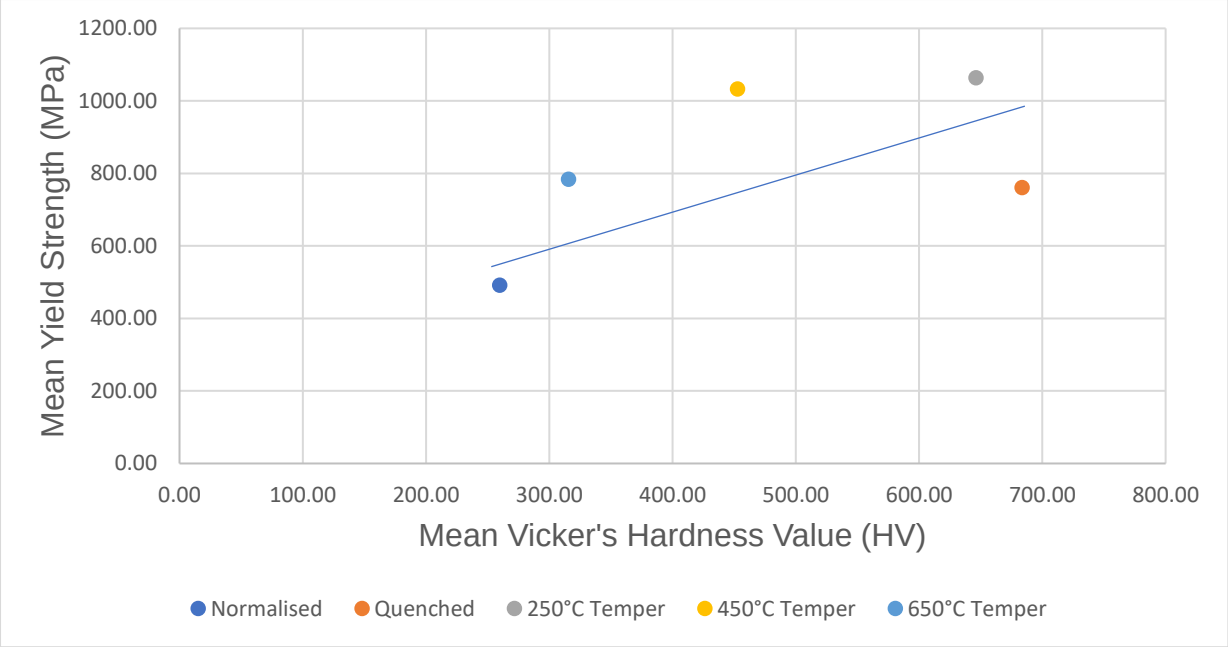

Figure 12: Graph to show the correlation between tensile strength and hardness value.

However, the quenched specimens with highest hardness shows the second lowest average yield strength with 761.1296MPa. This low strength could be explained by the large standard deviation, of 323.3726, where the sum of average yield strength and standard deviation would equal the largest yield strength of 1084.5022MPa.

A comparison between the ASTM A370 and experimental data, for stress against Vicker's hardness, is shown on Fig. 13.

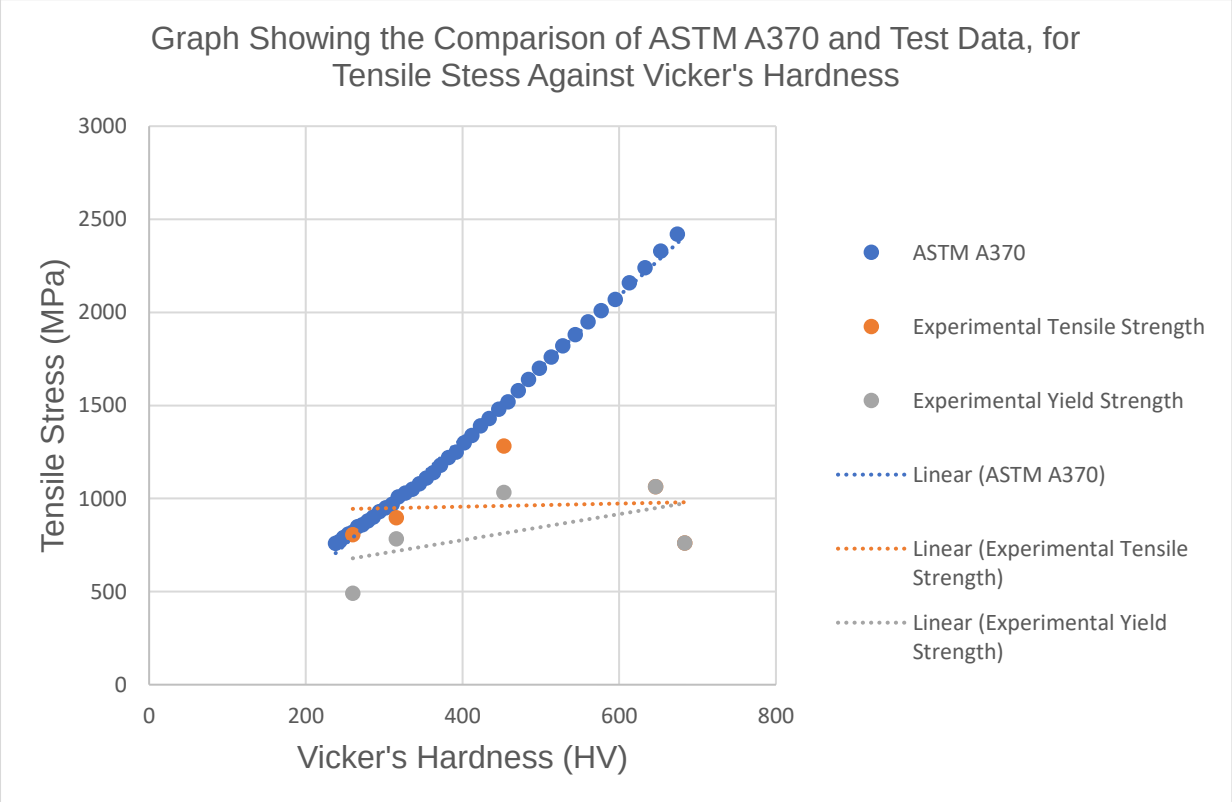

Figure 13: Graph to show comparison between the ASTM A370 and experimental data.

Vicker's Hardness Test

From the hardness results the quenched specimens have the highest hardness, then the tempered specimens (from lowest tempering temperature to highest) and then the normalised specimens.

During the austenisation state of steel in the furnace, the crystal structure of the iron transforms from BCC to FCC. This change in crystal structure of the steel allows the carbon to diffuse into the FCC iron crystal, as the FCC octahedral sites are larger than the BCC tetrahedral sites (Callister & Rethwisch, 2014). When quenched the rapid cooling quickly changes the iron structure back to BCC. There is not enough space for the carbon to diffuse out of the structure between the iron atoms, so the carbon remains and creates an extremely hard and brittle solution called martensite. These carbon particles catch the slip of the dislocation in the crystal structure when stressed and prevents further slip, this is called interstitial solid solution hardening. (Brush-Wellman-Inc, 2010)

During the tempering processes the elevated heat allows some carbon atoms to diffuse out of the martensite to create tempered martensite. This reaction follows the equation:

Martensite (BCT, single phase) —> Tempered martensite (α + Fe_3C phases)
(Callister & Rethwisch, 2014)

Due to rate of diffusion being dependent on heat, also shown in equation 2, the higher tempering temperature results in greater amounts on carbon diffused out of the crystalline structure. This loss of carbon then results in a loss of hardness. The normalised specimens have the lowest hardness at 259.88HV as there is no martensite. Due to the slow air cooling the carbon atoms diffuse from the grain crystal to create ferrite with cementite boundaries.

Mechanical Properties to Grain Structure Relationship

The EBSD microscopy could not be completed due to the Covid-19 situation. However, the relationship between the grain structure and mechanical properties of heat-treated steel was researched is presented below. The Hall-Petch relation correlates the strength of a material with the grain size. The smaller the grain size produces a greater grain boundary density, which results in a greater stress required to move a dislocation across the grain (Materion.com, 2010).

It is shown that the faster the cooling rate of a ferritic steel the finer the resulting grain size is (Umemoto et al. 1987). So, from this it would be expected that the quenched specimens would have the finest grain size. When this is then applied to the Hall-Petch relation, the quenched specimens should have the highest yield strength. The phases of the specimens would have also been examined. The phases of a steel can be predicted by a time-temperature transformation (TTT) curve. The curve presents the time and temperature to start and finish the transformation to a transformation product or phase (MacKenzie, 2018).

Using a TTT curve it can be predicted that from the graph and test specimens, that the quenched specimens would show a martensitic phase due to the rapid cooling and the normalised specimens would show ferrite and pearlite phases. The tempered specimens would initially show martensite after quenching and then after

tempering would presents tempered martensite which would be small cementite particles in a ferrite matrix (Callister & Rethwisch, 2014).

Conclusions

From the experimental procedure taking into account all limitations and flaws identified, it can be concluded that:

- As the tempering temperature increases the ductility and toughness of the medium carbon steel increases, with an additional average of 47.1J of energy absorbed from 250°C temper to 450°C temper then 650°C temper.
- Different heat treatments cause no significant variation in the tensile modulus of the medium carbon steel.
- A confirmation of strength-hardness relation for EN9 steel which indicates a positive increase in hardness from heat treatment correlates to an increase of yield strength.
- A confirmation of the Hall-Petch relation for EN9 steel which indicates a positive increase of yield stress to the finer the grains. However, this is less significantly correlating when comparing the grain size to tensile strength.
- EN9 steel is not affected by tempering embrittlement.

Recommendations

For further development of the research and paper I would make the following recommendations:

- To repeat the study and ensure actual EBSD microscopy data is collected, to enable complete comparisons between the actual grain structure and mechanical properties.
- Further repeats of the experimental procedure with an increased number of specimens to obtain more accurate results and lower the coefficient of variation of test parameters.
- Research into additional heat treatment procedures to allow greater comparison and insight into how heat treatments effect the grain structure and mechanical properties.

Acknowledgments

I would like to thank my supervisors Dr Alistair Cree and Dr Dan Haspel for their help and guidance to complete this paper.

I would also like to thank Mr. Terry Richards and Dr Jeremy Clark for their assistance and advice to complete the experimental testing.

To Mr Neil Fewings for the manufacturing of the test specimens.

And finally, to my family and friends who encouraged and supported me.

Nomenclature

- BCC – Body centred cubic
- FCC – Face centred cubic
- BCT – Body centred tetragonal
- FEPA - Federation of European Producers of Abrasives
- EBSD – Electro backscatter diffraction
- SEM – Scanning electron microscope
- TTT – Time-temperature transformation
- CAD – Computer aided design
- EN – Emergency number
- %wt – Weight percentage
- $\sigma(d)$ – Stress at Yield
- σ_0 – Corresponding stress
- k_{HP} – Material constant
- d – Grain size
- F – Force
- D - Arithmetic mean of the two diagonal lengths of the imprint
- °C – Degree Celsius
- mm - Millimetre
- µm - Micrometres
- m/s – Metres per second
- mm/min – millimetres per minute
- HV – Hardness value
- J – Joule
- kV – Kilovolts
- nA – Nanoamps
- MPa – Megapascal
- GPa – Gigapascal
- mb - Millibar
- PSI – Pounds per square inch

References

ASTM-International. (2016, 07 15). *Standard Test Methods for.* Retrieved from 3ppars.com: https://www.3ppars.com/WebsiteImages/download/48152874911.PDF

Boyer, H. E., P 3, 19, 91, 109 (1984). *Practical Heat Treating.* American Society for Metals.

Brush-Wellman-Inc. (2010, 04 16). *Solid Solution Hardening & Strength.* Retrieved from materion.com: https://materion.com/-/media/files/alloy/newsletters/technical-tidbits/issue-no-16-solid-solution-hardening--strength.pdf

Callister, W. D., & Rethwisch, D. G., P 233, 300, 301, 364, 365, 416, 417, 419, 591 (2014). *Materials Science and Engineering.* John Wiley and Sons.

Driscoll, J. R. (2014, 12 01). *The effect of tempering parameters on the hardness and precipitation.* Retrieved from The University of Birmingham: https://etheses.bham.ac.uk/id/eprint/8336/1/Driscoll18MScbyRes.pdf

ebsd.com. (2020a). *Introduction*. Retrieved from ebsd.com: http://ebsd.com/hints-tips-for-ebsd-data-collection/ebsd-sample-preparation/introduction

ebsd.com. (2020b). *Sample mounting*. Retrieved from ebsd.com: http://ebsd.com/hints-tips-for-ebsd-data-collection/ebsd-sample-preparation/sample-mounting

ebsd.com. (2020c). *Polishing*. Retrieved from ebsd.com: http://ebsd.com/hints-tips-for-ebsd-data-collection/ebsd-sample-preparation/polishing

Fedotov, I. F. (2011, 04 21). A mathematical model of laser surface heat-cooling treatment for medium carbon steel. *Journal of the Southern African Institute of Mining and Metallurgy*. Retrieved from http://www.scielo.org.za/scielo.php?script=sci_arttext&pid=S2225-62532011000600003

Hashemi, S. H. (2010). Strength–hardness statistical correlation in API X65 steel. *Materials Science and Engineering A*, 1652.

Kalpakjian, S., & Schmid, S. R., P 57, 109, 110, 237 (2003). *Manufacturing Processes for Engineering Materials.* Pearson Education, inc.

Lee, S.-J., Matlock, D. K., & Van Tyne, C. J. (2011). An Empirical Model for Carbon Diffusion in Austenite. *ISIJ International*, 1903.

Lement, B. S., Averbach, B. L., & Cohen, M. (1955). *Further Study of Microstructural Changes on Tempering Iron Carbon Alloys.*

Li, Y., & Dunstan, D. (2019). *The Hall-Petch effects as a manifestation of the general size effect.* Queen Mary University of London.

MacKenzie, D. (2018, 09 15). *The Time-Temperature-Transformation Curve*. Retrieved from gearsolutions.com: https://gearsolutions.com/departments/hot-seat/the-time-temperature-transformation-curve/

Materion.com. (2010, 03 15). *Grain Size and Material Strength*. Retrieved from materion.com: https://materion.com/-/media/files/alloy/newsletters/technical-tidbits/issue-no-15---grain-size-and-material-strength.pdf

Midea, S. J. (2016, 05 09). *Design and Development of PPAP-Ready Wheel-Bearing Inductors*. Retrieved from www.industrialheating.com: https://www.industrialheating.com/articles/92865-design-and-development-of-ppap-ready-wheel-bearing-inductors

NSAI-Standards. (2018, 03 07). *NSAI-Standards.* Retrieved from Metallic materials - Vickershardness test: https://infostore.saiglobal.com/preview/is/en/2006/i.s.eniso6507-1-2018.pdf?sku=557814

Oxford-Instruments. (2020a). *Microstructure Visualization in SEM*. Retrieved from Oxford Instruments: http://www.ebsd.com/solving-problems-with-ebsd/microstructure-visualization-in-sem#grain-boundary-characterisation

Roberts , C. S., Averbach, B. L., & Cohen, M. (1953). *The Mechanism and Kinetics of the First Stage of Tempering.*

Storer-Adam, R. (2019, 11 25). *The history of case hardening and its processes*. Retrieved from Double Stone Steel: https://www.doublestonesteel.com/blog/metal-blog/the-history-of-case-hardening-and-its-processes/

TATA-STEEL. (2015). *Engineering Bar Product Manual.* Retrieved from TATA STEEL: https://www.tatasteeleurope.com/static_files/Downloads/Services/Service%20Centres/Distribution%20UKandI/tata-steel-distribution-engineering-bar-product-manual-ENG.pdf

Technical-Tidbits. (2010, 04 16). *Solid Solution Hardening & Strength.* Retrieved from Technical Tidbits: https://materion.com/-/media/files/alloy/newsletters/technical-tidbits/issue-no-16-solid-solution-hardening--strength.pdf

TWI. (2020). *WHAT IS TEMPER EMBRITTLEMENT, AND HOW CAN IT BE CONTROLLED?* Retrieved from TWI: https://www.twi-global.com/technical-knowledge/faqs/faq-what-is-temper-embrittlement-and-how-can-it-be-controlled

Umemoto, M., Zing Hai Guo, & Tamura, I. (1987). Effect of cooling rate on grain size of ferrite in a carbon steel. *Materials Science and Technology*, 254.

www.britannica.com. (2020). *Elasticity*. Retrieved from www.britannica.com: https://www.britannica.com/science/elasticity-physics

www.buehler.co.uk. (2020). *Grinding and Polishing Guide*. Retrieved from www.buehler.co.uk: https://www.buehler.co.uk/grinding-and-polishing-guide.php

www.ebsd.com. (2020). *Introduction*. Retrieved from www.ebsd.com: http://www.ebsd.com/ebsd-explained/11-home

www.metalspiping.com. (2016, 05 1). *Standard Test Methods and Definitions for.* Retrieved from http://www.metalspiping.com/: http://www.metalspiping.com/wp-content/uploads/2017/12/astm-a370-asme-sa-370.pdf

www.steelexpress.co.uk. (2020). *EN9 Steel*. Retrieved from www.steelexpress.co.uk: https://www.steelexpress.co.uk/engineeringsteel/EN9.html

www.twi-global.com. (2020). *AUSTENITE MARTENSITE BAINITE PEARLITE AND FERRITE STRUCTURES*. Retrieved from www.twi-global.com: https://www.twi-global.com/technical-knowledge/faqs/faq-what-are-the-microstructural-constituents-austenite-martensite-bainite-pearlite-and-ferrite

Appendices are available as 'supplementary files' (please see download area)